Biochemistry and Biophysics Reports 40 (2024) 101854

Contents lists available at ScienceDirect

Biochemistry and Biophysics Reports

journal homepage: www.elsevier.com/locate/bbrep

An *in-silico* approach to target multiple proteins involved in anti-microbial resistance using natural compounds produced by wild mushrooms

Gagandeep Singh [a,b,1], Md Alamgir Hossain [c,1], Dhurgham Al-Fahad [d], Vandana Gupta [e], Smriti Tandon [a], Hemant Soni [a], Cheemalapati Venkata Narasimhaji [a], Mariusz Jaremko [f], Abdul-Hamid Emwas [g], Md Jamir Anwar [h], Faizul Azam [i,*]

[a] *Section of Microbiology, Central Ayurveda Research Institute, Jhansi, Uttar Pradesh, India, 284003*
[b] *Kusuma School of Biological Sciences, Indian Institute of Technology Delhi, New Delhi, India, 110016*
[c] *Department of Pharmacy, Jagannath University, 9, 10 Chittaranjan Ave, Dhaka, 1100, Bangladesh*
[d] *Department of Pharmaceutical Sciences, College of Pharmacy, University of Thi-Qar, Iraq*
[e] *Departments of Microbiology, Ram Lal Anand College, University of Delhi, Benito Juarez Road, New Delhi, 110021, India*
[f] *Smart-Health Initiative (SHI) and Red Sea Research Center (RSRC), Division of Biological and Environmental Sciences and Engineering (BESE), King Abdullah University of Science and Technology (KAUST), Thuwal, 23955-6900, Saudi Arabia*
[g] *Core Labs, King Abdullah University of Science and Technology (KAUST), Thuwal, 23955-6900, Saudi Arabia*
[h] *Department of Pharmacology and Toxicology, College of Pharmacy, Qassim University, Buraydah, 51542, Saudi Arabia*
[i] *Department of Medicinal Chemistry and Pharmacognosy, College of Pharmacy, Qassim University, Buraydah, 51452, Saudi Arabia*

ARTICLE INFO

Keywords:
Anti-microbial resistance
Multi-drug resistance
Mushroom compounds
Molecular docking
Molecular dynamics

ABSTRACT

Bacterial resistance to antibiotics and the number of patients infected by multi-drug-resistant bacteria have increased significantly over the past decade. This study follows a computational approach to identify potential antibacterial compounds from wild mushrooms. Twenty-six known compounds produced by wild mushrooms were docked to assess their affinity with drug targets of antibiotics such as penicillin-binding protein-1a (PBP1a), DNA gyrase, and isoleucyl-tRNA synthetase (ILERS). Docking scores were further validated by multiple receptor conformer (MRC)-based docking studies. Based on the MRC-based docking results, eight molecules were short-listed for ADMET analysis. Molecular dynamics (MD) simulations were further performed to evaluate the conformational stability of the ligand-protein complexes. Binding energies were computed by the gmx_MMPBSA method. The data were obtained in terms of root-mean square deviation, and root-mean square fluctuation justified the stability of Austrocortilutein A, Austrocortirubin, and Confluentin in complex with several proteins under physiological conditions. Among these, Austrocortilutein A displayed better binding affinity with PBP1a and ILERS when compared with their respective reference ligands. This study is preliminary and aims to help drive the search for compounds that have the capacity to overcome the anti-microbial resistance of prevalent bacteria, using natural compounds produced by wild mushrooms. Further experimental validation is required to justify the clinical use of the studied compounds.

1. Introduction

Antibiotics are classified mainly according to their mechanism of action, which includes cell wall synthesis inhibitors, protein synthesis inhibitors, nucleic acids synthesis inhibitors, and antimetabolites [1]. Antibiotics exhibit their activity by inhibiting these pathways when interacting with the specific cell proteins responsible for specific actions [2]. Anti-microbial agents that act on the cell wall are supposed to be selective and provide a high therapeutic index. This group of antibiotics resists the synthesis of the peptidoglycan layer that ultimately leads to the lysis of the cell [3]. Different antibiotics of this group express their activity in various stages of peptidoglycan biosynthesis, such as in the cytoplasmic, membrane, and periplasmic space, while β-Lactams is active in the exterior portion of the cell stratum in the periplasmic space. These antibiotics have a β-lactam ring that interacts with penicillin-binding proteins (PBPs) and terminate their biological activity

* Corresponding author.
E-mail address: f.azam@qu.edu.sa (F. Azam).
[1] Both authors have made equal contributions.

https://doi.org/10.1016/j.bbrep.2024.101854
Received 20 September 2024; Received in revised form 15 October 2024; Accepted 17 October 2024

Table 1
Grid coordinates of the box used for blind docking of compounds on 3TTZ, 3UDX, and 1JZS proteins.

3TTZ		3UDX		1JZS	
Center (Å)	Box Size (Å)	Center (Å)	Box Size (Å)	Center (Å)	Box Size (Å)
x = 11.23	x = 55.58	x = −32.66	x = 95.27	x = −24.35	x = 105.33
y = 11.52	y = 52.94	y = 46.01	y = 138.70	y = 4.85	y = 81.05
z = 21.55	z = 59.10	z = −7.46	z = 79.08	z = −20.82	z = 119.92

[4]. Fosfomycin inhibits the conversion of enolpyruvate to intermediate uridine diphosphate-N-acetylglucosamine (UDP-NAG) in the membrane stage. D-cycloserine is a promising inhibitor of alanine racemase (Alr) and D-alanyl-D-alanine synthetase (Ddl) that engages in the cytoplasmic stage, ultimately inhibiting the assimilation of Ddl in UDP-N-acetylmuramic acid (UDP-NAMA) [5]. The PBP1a encoding gene has been identified to be crucial for the pathogenicity of group *B streptococcus* [6]. It induces bacterial cell division by directly interacting with the multiprotein divisome complex [7], and mutations in PBP1a confer a greater level of resistance in *S pneumoniae* to the antibacterial action of penicillin [8]. Further, beta lactams such as penicillin and cephalosporins exhibited PBP1a as a preferential target for antibacterial action [9]. Also, the median infectious dose (ID_{50}) of many bacterial strains was lower for PBP1a than other PBPs [10], suggesting that it might be a suitable target for mitigating bacterial resistant to β-lactam antibiotics. Antibiotics inhibiting protein synthesis usually distress bacterial ribosomes through interactions with 30S and/or 50S subunits [11]. Macrolides, chloramphenicol, and oxazolidones act in the 50S subunit, while aminoglycosides, tetracyclines, and nitrofuran bind the 30S subunit. Chloramphenicol exerts its activity by interfering with tRNA binding and inhibition of peptidyl transferase, thus resisting protein chain elongation [12,13]. Another antibiotic acting on protein synthesis is mupirocin, which terminate the activity of isoleucyl-tRNA synthetase (ILERS). The emergence of methicillin-resistant *S. aureus* (MRSA) strains poses challenges to antimicrobial therapy, and about 13.8 % of MRSA strains have also developed resistance to mupirocin, which acts by inhibiting isoleucyl-tRNA synthetase [14]. Isoleucyl-tRNA synthetase could be an excellent target to overcome such antimicrobial resistance, which is due to mutations in genes that induce alterations in the HIGH (His-Ile-Gly-His) motif, as well as by acquisition of a resistant gene (*ileS* gene) from DNA viruses [15]. Quinolones are synthetic anti-microbial compounds that interfere with DNA synthesis through the inhibition of DNA gyrase which induces negative supercoils to relieve the stress in the DNA helix during replication and transcription [16]. mRNA synthesis is inhibited by Rifampicin which causes malfunctioning of RNA polymerase. Surprisingly, mutations in the DNA gyrase gene have resulted in an alarming increase in fluoroquinolone resistance among *Enterobacteriaceae* [17], revealing DNA gyrase as a novel target for antimicrobial drugs.

Antibiotic resistance has become a global health issue, and diseases induced by multidrug-resistant bacteria are rising alarmingly Consequently, antibiotic resistance is recognized as a critical global health

Table 2
Docking score of the native crystal ligands attached to the target proteins. The scores were set as cut-offs for the respective proteins with respect to selection of anti-microbial agents.

Native crystal ligands	Protein PDB ID	Docking score (Kcal/mol)
IM2	3UDX	−6.2
07 N	3TTZ	−6.8
MRC	1JZS	−6.7

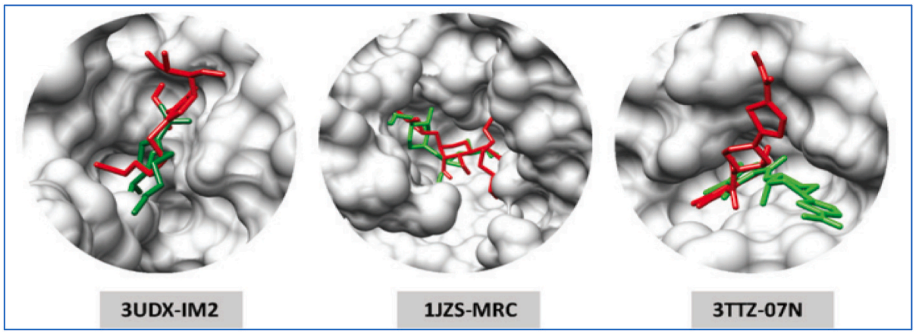

Fig. 1. The superimposed representation of the native inhibitors in the crystal (green) and virtually docked (red) form. (For interpretation of the references to color in this figure legend, the reader is referred to the Web version of this article.)

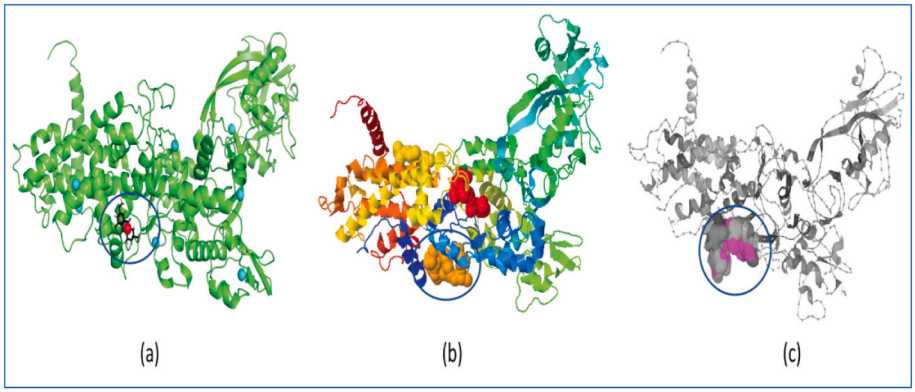

Fig. 2. Identification of an allosteric binding site in 1JZS by (a) PARS, (b) PASSER, and (c) Prank web servers.

Table 3
Docking score of 26 anti-microbial agents from a wild mushroom with three different target proteins. Yellow indicates similar binding affinity, red indicates lower binding affinity, and green indicates higher binding affinity of the compounds compared with the reference ligands. Only green-colored molecules were shortlisted.

S.No.	Compounds	3UDX	3TTZ	1JZS
1	2,4-Dihydroxy-benzoic acid	-5.8	-5.6	-5.8
2	2-Aminoquinoline	-6.4	-6.1	-6.2
3	Austrocortilutein A	-7.1	-8.1	-8
4	Austrocortirubin	-7.4	-7.2	-8.5
5	Caffeic acid	-6.1	-6.6	-5.8
6	Chlorogenic acid	-7.2	-7.2	-8.3
7	Cinammic	-7	-6.8	-7.1
8	Coloratin A	-7	-7	-7.2
9	Confluentin	-7.8	-7.1	-7.8
10	Ellagic acid	-8	-8.7	-8.9
11	Emodin	-7.3	-8.3	-8.5
12	Erythroglaucin	-7.9	-8.2	-8.1
13	Ferulic acid	-5.4	-5.9	-5.7
14	Gallic acid	-5.6	-6	-6.3
15	Ganomycin A	-5.8	-6.3	-6.5
16	Ganomycin B	-5.4	-6.9	-6.2
17	Grifolin	-6.1	-5.4	-5.7
1	Neogrifolin	-6.7	-6.5	-5.7
8	o-Coumaric acid	-6.1	-6.2	-6
19	Oxalic acid	-4.1	-4.2	-4
20	p-Coumaric acid	-5.6	-6.1	-5.9
21	Physcion	-7.6	-8.3	-8.1
22	Protocatechuic acid	-5.4	-5.9	-5.5
23	Quercetin	-8.7	-8.3	-8.4
24	Syringic acid	-5.7	-5.7	-5.6
25	Torosachrysone	-7.7	-8.1	-8
26	Vanillic acid	-5.4	-5.7	-5.8

Table 4
MRC docking of ligands with PBP1a.

Compounds	3UDF	3UDI	3UE0	3UE1
2-Aminoquinoline	-6	-6.3	-6.2	-6.1
Austrocortilutein A	-7	-8	-7.9	-7.6
Austrocortirubin	-6.9	-7.5	-7.6	-7.2
Chlorogenic acid	-7.4	-7.3	-7.3	-6.9
Cinammic	-7	-7	-7	-6.8
Coloratin A	-6.7	-6.6	-7.1	-6.8
Confluentin	-7.8	-7.4	-7.5	-7.7
Ellagic acid	-7.8	-8.1	-8	-8.2
Emodin	-7.4	-7.4	-7.4	-7.7
Erythroglaucin	-6.9	-7.2	-7.1	-7.3
Neogrifolin	-7.1	-6.5	-6.1	-6.9
Physcion	-7.1	-7.2	-7.5	-7.5
Quercetin	-8.2	-8.1	-8.2	-8.4
Torosachrysone	-7.1	-7.2	-6.8	-7

Table 5
MRC docking of ligands with DNA gyrase.

Compounds	3RAD	3RAF	4KOE	4Z4Q
AustrocortiluteinA	-7	-7.9	-7.2	-7.4
Austrocortirubin	-7.5	-7.7	-7.2	-7.3
Chlorogenic acid	-7.1	-6.7	-6.8	-8.1
Coloratin A	-5.9	-6.8	-6	-6
Confluentin	-5.9	-6	-6.4	-7.8
Ellagic acid	-8	-7.2	-7.4	-8.3
Emodin	-7.5	-7.2	-6.8	-7.9
Erythroglaucin	-7	-7.3	-6.7	-8
Ganomycin B	-6.2	-5.1	-5.9	-6.8
Physcion	7.1	-7.2	-7.8	-7.7
Quercetin	-8.1	-8.1	-7.2	-8.4
Torosachrysone	-6.8	-7.4	-7.4	-8

crisis which threatens the effectiveness of antibiotics and other antimicrobial drugs in treating bacterial infections [18]. In Europe alone, about 25,000 people die due to multidrug-resistant bacterial infections. On the other hand, in America, nearly 2 million people are affected, with around 23,000 mortalities [19]. Due to this emerging problem, it is essential to search for new antibiotics from natural sources that could act alone and in combination with existing drugs to enhance their efficacy and reduce the development of resistance to antimicrobial agents. Mushrooms contain diverse bioactive compounds and have a long history of traditional use to combat infections, cleanse the blood, restore the liver, expel kidney stones, prevent and heal cancers, among other indications, and are recognized also by modern science as a good source of potent anti-microbial agents [20,21]. It is intriguing that various extracts from G. lucidum mycelia exhibited antimicrobial activity against *E. coli*, *P. aeruginosa*, *S. aureus*, and *S. pyogenes* [22]. Additionally, the ethanolic and aqueous extracts from the fruiting bodies of

Table 6
MRC docking of ligands with ILERS.

Compounds	1JZQ	1OBH
AustrocortiluteinA	-7.3	-6.7
Austrocortirubin	-7.4	-7.2
Chlorogenic acid	-7.8	-6.6
Cinammic	-7.2	-6.5
Coloratin A	-7.1	-6.1
Confluentin	-8.3	-6
Ellagic acid	-8.3	-8
Emodin	-8.7	-7.2
Erythroglaucin	-8.7	-7
Physcion	-7.4	-7.1
Quercetin	-8.2	-7.7
Torosachrysone	-7.5	-6.8

P. ostreatus demonstrate antimicrobial activity against *S. aureus* and *E. coli* [23]. However, the action mechanisms of mushroom compounds are not clear and require further investigation [24]. The research reported here aims to contribute to our understanding of the action mechanisms of a few selected species of mushrooms and help us identify antibacterial compounds in these mushrooms. For this purpose, we applied a computer-aided drug design (CADD) approach, including molecular docking, multiple receptor conformer (MRC) based docking, drug-likeness and ADMET analysis, as well analysis of drug interactions with target proteins, further supported by MD simulation analysis. A classical MD was employed to investigate the dynamic behavior and stability of protein-ligand complexes over time. Classical MD is a well-established method that treats atoms and molecules as classical particles, using force fields to describe interactions such as bond lengths, angles, and van der Waals forces [25]. This approach is highly efficient, allowing for the simulation of large biomolecular systems on extended time scales, making it ideal for understanding processes like protein-ligand binding and conformational changes [26,27]. However, while classical MD is effective for studying dynamic processes, it does not capture the quantum-level electronic interactions within a system, which can be addressed through Density Functional Tight Binding (DFTB) methods. Recent studies have demonstrated that DFTB can offer more precise predictions of binding energies and molecular interactions at the quantum level, surpassing the capabilities of classical MD in this respect [28,29]. Despite these advantages, classical MD remains a valuable tool for exploring molecular interactions in larger systems over longer periods, as it allows for extensive sampling of molecular motions that are important for understanding how proteins interact with ligands over time [30,31].

2. Material and methods

2.1. Selection of proteins

The target protein structures PDB: 3UDX (X-ray structure, 2.50 Å) for penicillin-binding protein 1a (PBP1a) of *Acinetobacter baumannii*, PDB: 3TTZ (X-ray structure, 1.63 Å) for DNA gyrase of *Staphylococcus aureus*, and PDB: 1JZS (X-ray structure, 2.50 Å) for isoleucyl-tRNA synthetase (ILERS) of *Thermus thermophilus* were selected from the RCSB database (https://www.rcsb.org/). PBP1a is involved in cell wall synthesis, DNA gyrase in nucleic acid, and ILERS in protein synthesis. Although *T. thermophilus* is not a pathogenic bacterium but mupirocin which is present as a co-crystal in PDB: 1JZS, it is a selective inhibitor of the archaeal and eubacterial ILERS but not the eukaryotic enzymes. Mupirocin is used in clinics to treat methicillin-resistant *Staphylococcus aureus* infections. As the binding pocket and interacting residues are conserved in *T. thermophilus* and pathogenic eubacteria, we used its crystal structure as available in the Protein DataBase [32]. No other mupirocin-bound suitable structure from a pathogenic bacterium is available from PDB.

2.2. Preparation of proteins

The crystal structure of proteins with PDB IDs 3UDX, 3TTZ, and 1JZS were retrieved from the RCSB protein databank (PDB) [33]. All the proteins were prepared by removing attached crystallographic water, heteroatoms, and ligands using PyMOL [34]. PDB:3TTZ and PDB:3UDX had missing loops with more than 30 amino acids which were difficult to model as most software that can add missing loops can do so reliably only for small gaps, maximally up to 15–20 amino acids. Moreover, the missing loop region is not falling within the active site used for docking, nor does it contribute to the docking pocket surface and was therefore ignored. Polar hydrogens and Gasteiger charges were added by AutoDockTools-1.5.6 [35]. The titratable amino acids in the target proteins were protonated to be suitable for pH 7.4. The output files were saved in the PDBQT format required for molecular docking.

2.3. Preparation of ligands

Twenty-six compounds from wild mushrooms predicted to have antimicrobial properties were selected as ligands [21]. Their 3D structures were downloaded in SDF format from the NCBI PubChem database [36] and converted to PDB format using PyMOL. The ligands were protonated to be suitable for pH 7.4, and energy minimizations of these ligands were done by AutoDockTools-1.5.6 and saved in PDBQT format for docking [37].

2.4. Molecular docking

To investigate the affinity of the ligands, blind molecular docking was done for all the compounds using AutoDock Vina [38]. The grid coordinates, as listed in Table 1, were used for all three target proteins to cover the entire protein during blind docking. The exhaustiveness parameter was set to 100. The blind docking was carried out to check if the selected molecules have higher binding affinity to the possible allosteric sites in the proteins, other than the active sites. Moreover, the reference ligand present in the crystal structure of each protein was also re-docked with the target protein, and their binding affinity was taken as a standard to select the potent molecules having higher binding affinity than the reference ligands.

Table 7
Drug-likeness properties of molecules.

Attributes	Austrocortilutein A	Austrocortirubin	Confluentin	Emodin	Erythroglaucin	Physcion	Quercetin
Blood-Brain Barrier	BBB-	BBB-	BBB+	BBB+	BBB+	BBB+	BBB+
Human Intestinal Absorption	HIA+	HIA+	HIA+	HIA+	HIA+	HIA+	HIA+
P-glycoprotein Substrate	Substrate	Substrate	Substrate	Substrate	Substrate	Substrate	Substrate
P-glycoprotein Inhibitor	Non-inhibitor	Non-inhibitor	Non-inhibitor	Non-inhibitor	Non-inhibitor	Non-inhibitor	Non-inhibitor
CYP450 2C9 Substrate	Non-substrate	Non-substrate	Non-substrate	Non-substrate	Non-substrate	Non-substrate	Non-substrate
CYP450 2D6 Substrate	Non-substrate	Non-substrate	Non-substrate	Non-substrate	Non-substrate	Non-substrate	Non-substrate
CYP450 3A4 Substrate	Substrate	Substrate	Substrate	Non-substrate	Non-substrate	Non-substrate	Non-substrate
CYP450 1A2 Inhibitor	Inhibitor	Inhibitor	Inhibitor	Inhibitor	Inhibitor	Inhibitor	Inhibitor
CYP450 2C9 Inhibitor	Non-inhibitor	Non-inhibitor	Non-inhibitor	Inhibitor	Inhibitor	Non-inhibitor	Inhibitor
CYP450 2D6 Inhibitor	Non-inhibitor	Non-inhibitor	Non-inhibitor	Non-inhibitor	Non-inhibitor	Non-inhibitor	Non-inhibitor
CYP450 2C19 Inhibitor	Inhibitor	Non-inhibitor	Inhibitor	Non-inhibitor	Non-inhibitor	Non-inhibitor	Non-inhibitor
CYP450 3A4 Inhibitor	Non-inhibitor	Non-inhibitor	Non-inhibitor	Non-inhibitor	Non-inhibitor	Non-inhibitor	Non-inhibitor
CYP Inhibitory Promiscuity	Low	Low	Low	Low	Low	Low	Low
AMES Toxicity	Non-AMES toxic	Non-AMES toxic	Non-AMES toxic	AMES-toxic	AMES toxic	AMES toxic	AMES toxic
Carcinogenic	No	No	No	No	No	No	No
Acute Oral Toxicity	III	III	III	III	II	II	II

2.5. Multiple receptor conformer (MRC) based docking

To further validate the docking score, MRC-based docking was carried out on the different crystal structures of the target proteins from the same species for those compounds that were shortlisted after single target molecular docking. This was done to validate the interaction of the selected leads with target proteins of different conformations and to consider the inherent plasticity of the target proteins while performing molecular docking [39]. For this purpose, four crystal structures of PBP1a, four crystal structures of DNA gyrase, and another two crystal structures of ILERS were retrieved from the RCSB database. Crystal structures with ID(s) PDB:3UDF, PDB:3UDI, PDB:3UE0, and PDB:3UE1 were selected for PBP1a, PDB:3RAD, PDB:3RAF, PDB:4KOE, and PDB:4Z4Q for DNA gyrase, and PDB:1JZQ, and PDB:1OBH for ILERS were taken. After MRC docking, molecules were selected based on the specific cut-off values of re-docked reference molecules.

2.6. Drug-likeness and AMDET analysis

The properties of absorption, distribution, metabolism, excretion, and toxicity (ADMET) play an essential role in the drug discovery process, and the study of ADMET characteristics is an important tool in determining the *in vivo* pharmacokinetic properties of medicinal compounds. According to existing research, about 60 % of reported promising leads are excluded from clinical trials due to undesirable ADMET characteristics [40]. In this part of the study, physicochemical properties such as hydrogen bond acceptor, hydrogen bond donor, TPSA, lipophilicity, and water solubility (LogS) were assessed using Lipinski's rule of five, and pharmacokinetic parameters such as Blood-Brain Barrier (BBB) permeant, Human Intestinal absorption (HIA), Pgp substrate, and others were considered. Furthermore, various critical toxicity indices were assessed, such as acute oral toxicity, carcinogenicity, and AMES toxicity. The ADMET characteristics were investigated using the admetSAR web server [41].

Table 8
ADMET properties of the selected molecules.

Compounds	MW (g/mol)	RB	HBA	HBD	TPSA	LogP	LogS
Austrocortilutein A	304.29	1	6	3	104.06	1.84	-2.33
Austrocortirubin	320.29	1	7	4	124.29	1.94	-2.66
Confluentin	326.47	6	2	1	29.46	4.44	-5.85
Ellagic acid	302.19	0	8	4	141.34	0.79	-2.94
Emodin	270.24	0	5	3	94.83	1.81	-3.67
Erythroglaucin	300.26	1	6	3	104.06	2.47	-4.08
Physcion	284.26	1	5	2	83.83	2.49	-3.87
Quercetin	302.24	1	7	5	131.36	1.63	-3.16

Table 9
List of screened molecules subjected to MD simulations with the target proteins.

Screened molecules	Target Proteins			
	Austrocortilutein A	**3UDX**	**3TTZ**	**1JZS**
	Austrocortirubin	——	**3TTZ**	——
	Confluentin	**3UDX**	——	——

2.7. Superimposition of the co-crystal ligand with the docked ligand images

Superimposition of the co-crystal ligand with the docked ligand images was done using PyMol to visualize the deviation in docked pose of the co-crystal ligand from its experimentally determined binding pose and to validate the docking algorithm.

2.8. Binding interaction analysis

The docked views of the selected ligands with target proteins were analyzed using BIOVIA Discovery Studio 2019 [42]. The compounds Austrocortilutein A, Austrocortirubin, and Confluentin, in complex with their corresponding target proteins shown in Table 9, were further subjected to molecular dynamics simulations. The selection of compounds was based on their docking results, interactions with the active site residues, and AMDET filtering.

2.9. Molecular dynamics simulations

The molecular dynamics simulations for all three target proteins (PDB: 3UDX, 3TTZ, and 1JZS), alone and in combination with the screened and co-crystalized ligand molecules, were performed using LiGRO [43], a GUI based program for preparing systems for MD simulations, using GROMACS 5.1.5 package [44]. The system was solvated using the transferable intermolecular potential water molecules (TIP3P) model in a cubic box with the distance of each protein atom with the box edges being 1.5 nm, and periodic boundary conditions were used. The Amber FF99sb forcefield was used, and the system was neutralized with 0.15 M NaCl. The Amber FF99sb forcefield was used as it is extensively tested and validated against the NMR measurements, compatible with popular TIP3P water model, computationally efficient and widely used forcefield [45–47]. The General Amber Force Field (GAFF) and Ante Chamber PYthon Parser interfacE (ACPYPE) [48] tools were then used to define the parameters of the screened ligands. This system was equilibrated for 1ns each under the NVT ensemble at 310.15K and under the NPT ensemble at 1.01 bar using the modified Berendson thermostat and Parinello-Rehman barostat, respectively. The MD production for each system was run for 100ns at 310.15K and 1.01 bar. All the bonds with hydrogen atoms were constrained using the LINCS algorithm, and the electrostatic interactions were corrected by the Particle Mesh Ewald (PME) method. The integration time of 2fs was used, and the frames were stored after every 10ps. All the trajectories were visualized and analyzed using VMD, Chimera, and standard GROMACS tools. The binding free energy was calculated using gmx_MMPBSA software [49]. The MMGBSA calculations were performed for each complex using 100 frames isolated from the metastable region of 90–100ns of the trajectories. The GBOBC2 model (igb = 5) was chosen for MMGBSA calculations along with the internal dielectric constant value of 1. The total enthalpic contributions were estimated, including electrostatic, VDW, SASA, and polar solvation energies. The binding free energy contributions of respective positive control molecules were compared with the test molecules [49].

3. Results

3.1. Molecular docking

Fig. 1 shows the superimposed representation of crystal (green) and docked (orange) poses of co-crystallized inhibitor with RMSD less than 2 Å, which is generally acceptable [50]. The allosteric site in 1JZS was identified by different webservers (Fig. 2). Austrocortilutein A was found to be binding to the allosteric site of 1JZS (Fig. 2a). Docking scores of the reference ligands as well as the anti-microbial agents are given in Tables 2 and 3 respectively. Only the molecules exhibiting higher binding affinity (shown in green in Table 3) were selected for further

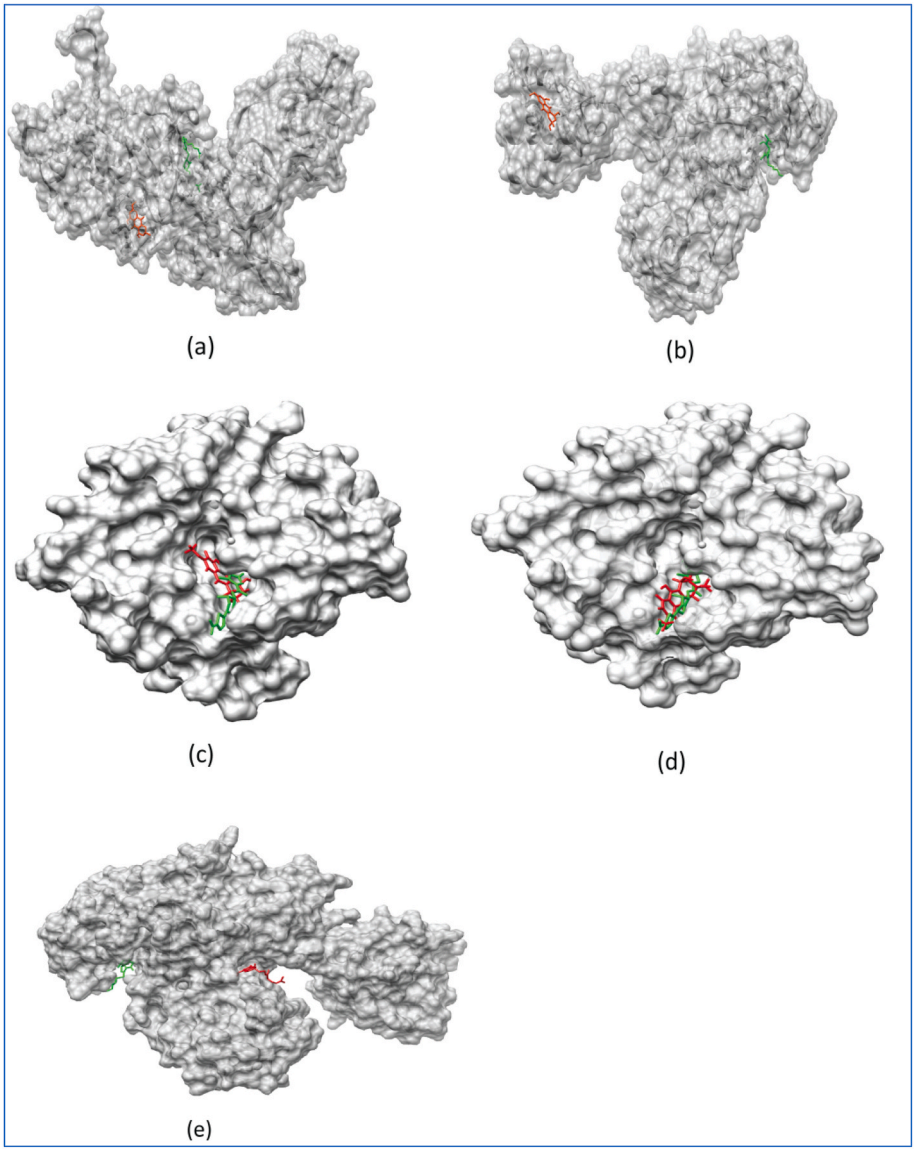

Fig. 3. Docked surface view representation of native crystal inhibitors (green) and Austrocortilutein A (orange) with (a) 1JZS, (b) 3UDX, (c) 3TTZ, and Austrocortirubin (orange) with (d) 3TTZ and Confluentin with (e) 3UDX. (For interpretation of the references to color in this figure legend, the reader is referred to the Web version of this article.)

studies.

For ILERS (PDB ID 1JZS), Austrocortilutein A was docked at an allosteric site, as predicted by the different webservers (Fig. 2). The residues lined by the allosteric cavity include Glu15, Leu18, Trp21, Lys22, Lys23, Lys25, Phe27, Gln28, Trp84, Glu127, Glu131, Thr134, Glu135, Tyr139, Trp140, Val141, Asp142, Leu143, and Glu144. Austrocortilutein A formed two conventional hydrogen bonds with Gln28 and Leu143, a C–H bond with Asp142, and multiple van der Waals interactions with residues Trp21, Lys22, Ile26, Glu131, Thr134, Glu135, Val141, along with π-alkyl and π-π T-shaped interactions with residues Lys25 and Phe27 respectively that might attune the activity of the protein by the allosteric modulations. The.

4. Multiple receptor conformer (MRC)-Based docking

In the MRC docking, the cut-off value was set to −7.0 kcal/mol for each group of proteins, and molecules having equal or higher binding capability with all the proteins of each group were selected, as shown in Tables 4–6. Table 4 shows Austrocortilutein A, Confluentin, Ellagic acid, Emodin, Physcion, and Quercetin were shortlisted for PBP1a protein because of compliance with the decided cut-off score criteria. In the case of DNA gyrase, as shown in Table 5, Austrocortilutein A, Austrocortirubin, Ellagic acid, Physcion, and Quercetin were selected as they showed an equal or higher binding affinity for all the proteins associated with DNA gyrase. Finally, for ILERS, Austrocortirubin, Ellagic acid, Emodin, Erythroglaucin, Physcion, and Quercetin were taken as they fulfilled the required cut-off criteria, as shown in Table 6. After merging the result of MRC-based docking, Austrocortilutein A, Austrocortirubin, Confluentin, Ellagic acid, Emodin, Erythroglaucin, Physcion, and Quercetin molecules were considered for further screening.

4.1. Drug likeness and ADMET Filtration

Drug likeness and ADMET properties of the selected molecules are given in Tables 7 and 8. According to Lipinski's rule of five, a molecule should have molecular weight ≤500, several hydrogen bond donors ≤5, a number of hydrogen bond acceptors ≤10, lipophilicity LogP ≤5, and a TPSA of no more than 140. Based on these values, Ellagic acid was withdrawn from the list due to its higher TPSA value, indicative of poor cell permeation ability (Table 7). The rest of the molecules had values in

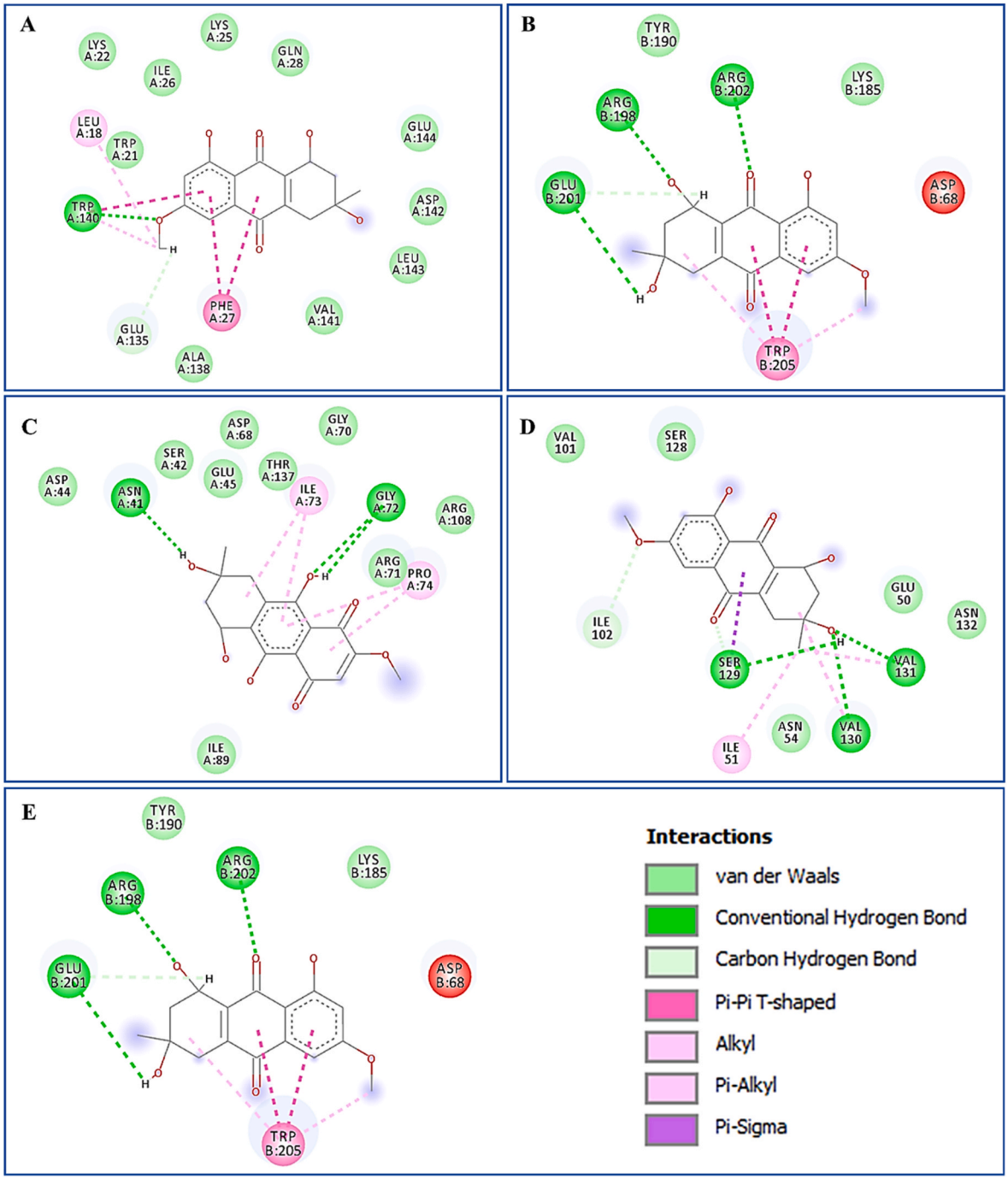

Fig. 4. 2D illustration of interaction of Austrocortilutein A with (a) 1JZS, (b) 3UDX, (c) 3TTZ, Austrocortirubin with (d) 3TTZ, and Confluentin with (e)3UDX.

the desirable range and were selected for further study.

ADMET analysis of the selected compounds reveal that all the molecules had the capability to cross the BBB except for Austrocortilutein A and Austrocortirubin. All of them can be absorbed from the intestine. Table 7 reveals that none of the compounds act as substrates for CYP2C9 or CYP2D6. However, Emodin, Erythroglaucin, and Quercetin inhibit CYP2C9, while the other compounds do not. Regarding CYP3A4, Austrocortilutein A, Austrocortirubin, and Confluentin are substrates, but none of the compounds inhibit this enzyme. Interestingly, all compounds inhibit CYP1A2, indicating a common inhibitory effect on this enzyme. Additionally, Austrocortilutein A and Confluentin inhibit CYP2C19, whereas the other compounds show no such inhibition. This suggests that while interactions with CYP2C9 and CYP2C19 are specific to a few compounds, CYP1A2 inhibition is a shared feature across all compounds. Additionally, Emodin, Erythroglaucin, Physcion, and Quercetin demonstrated AMES toxicity, leading to their exclusion from further studies.

4.2. *Binding interaction*

The docked pose and binding interactions of the three selected molecules, namely Austrocortilutein A, Austrocortirubin, and Confluentin, with different groups of proteins, are shown in Figs. 3 and 4. Austrocortilutein A interacts with the glycosyl transfer (TG) domain of PBP1a [51] through hydrogen bonding, van der Waals interaction, and other hydrophobic interactions. Arg198, Glu201, and Arg202 residues

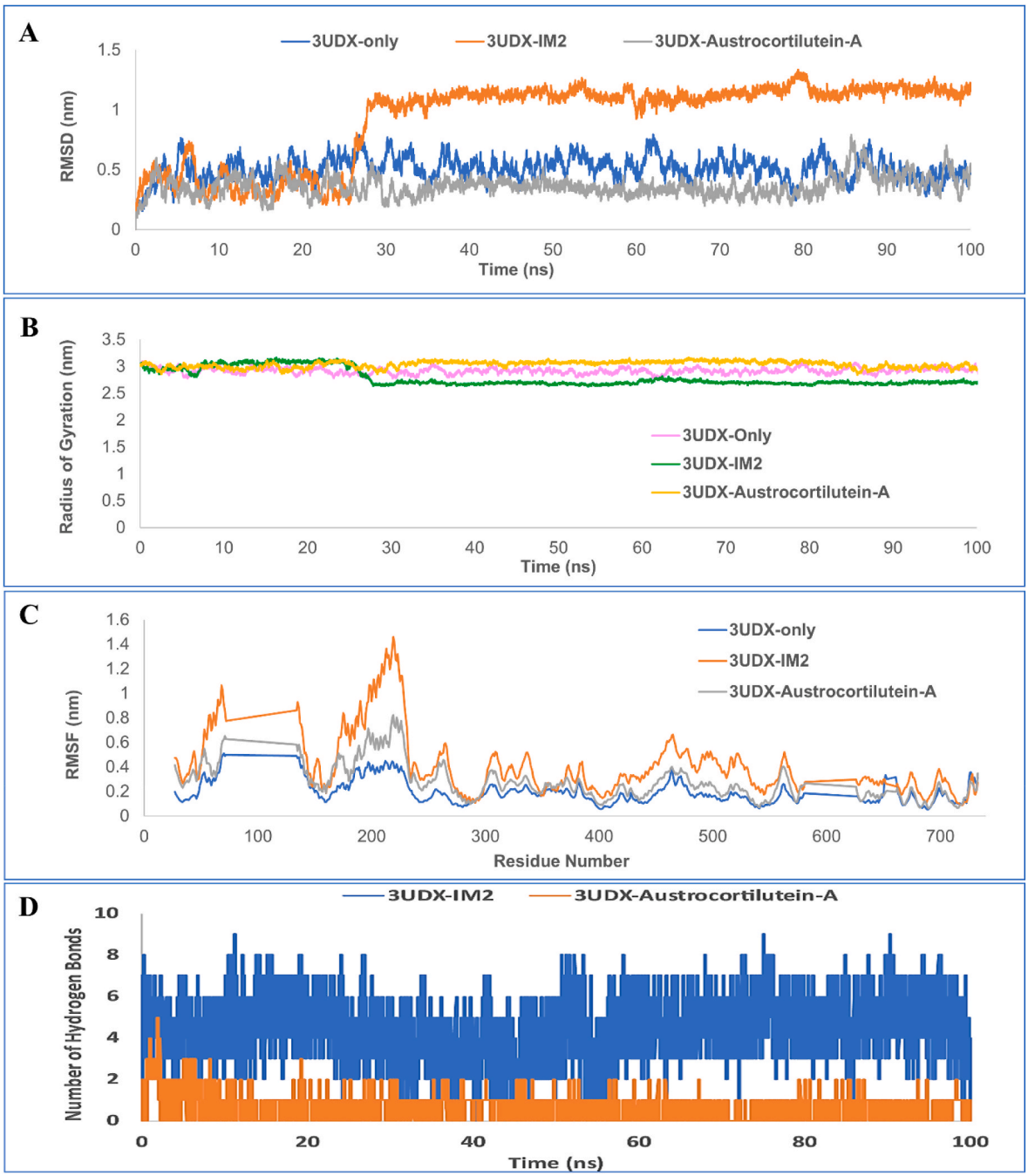

Fig. 5. Molecular dynamics (MD) simulation trajectory analysis of 3UDX-ligand complexes, (A) RMSD, (B) Radius of Gyration, and (C) RMSF and (D) Hydrogen Bonds. (Note: IM2 refers to the co-crystal ligand of 3UDX).

form a conventional hydrogen bond with Austrocortilutein A, while forming hydrophobic interactions with Lys185, Tyr190 and Trp205. The other screened molecule, Confluentin, interacts with the interdomain loops of the TP domain, OB domain, and the linker between the TG and TP domains. It forms a conventional hydrogen bond with Tyr415, π-anion interaction with Glu281, alkyl, and π-alkyl/σ interactions with Pro243, Tyr244 and Tyr418. It also forms van der Waals contacts with Asn240, Lys282, Gln285, Ala312, Tyr313, Ala314, Asn416, and Phe417. The binding of Confluentin at the interdomain junction could modulate the movement of these domains and, in turn, inhibit the function of this target protein [51].

For the ATP binding domain of DNA Gyrase B (PDB ID 3TTZ), the critical active site residues include Asp81, Arg84, Gly85, Arg144, and Thr173 [52]. Both Austrocortilutein A and Austrocortirubin interact with the crucial active site residues. Austrocortilutein A forms one conventional hydrogen bond with Asp81 and one carbon-hydrogen bond with Ser129. van der Waals interactions were established with Asn54, Ser55, Glu58, Gly83, Arg84, Gly85, Leu103, Ser128, Val130, Thr173, and Ile175. However, alkyl/pi-alkyl interactions were afforded by Ile86 and Ile102 residues. For Austrocortirubin, a conventional hydrogen bond forms with Arg84, along with hydrophobic interactions with residues Asn54, Ser55, Asp81, Gly83, Gly85, Ile102, Arg144, and Thr173, a Pi-anion interaction with Glu58 and alkyl/pi-alkyl interaction with the residues Ile86 and Pro87 of 3TTZ. These interactions of Austrocortilutein A and Austrocortirubin with the active site residues of DNA Gyrase B suggest their probable inhibitory potential, making them suitable candidates for further exploration as antibacterial compounds.

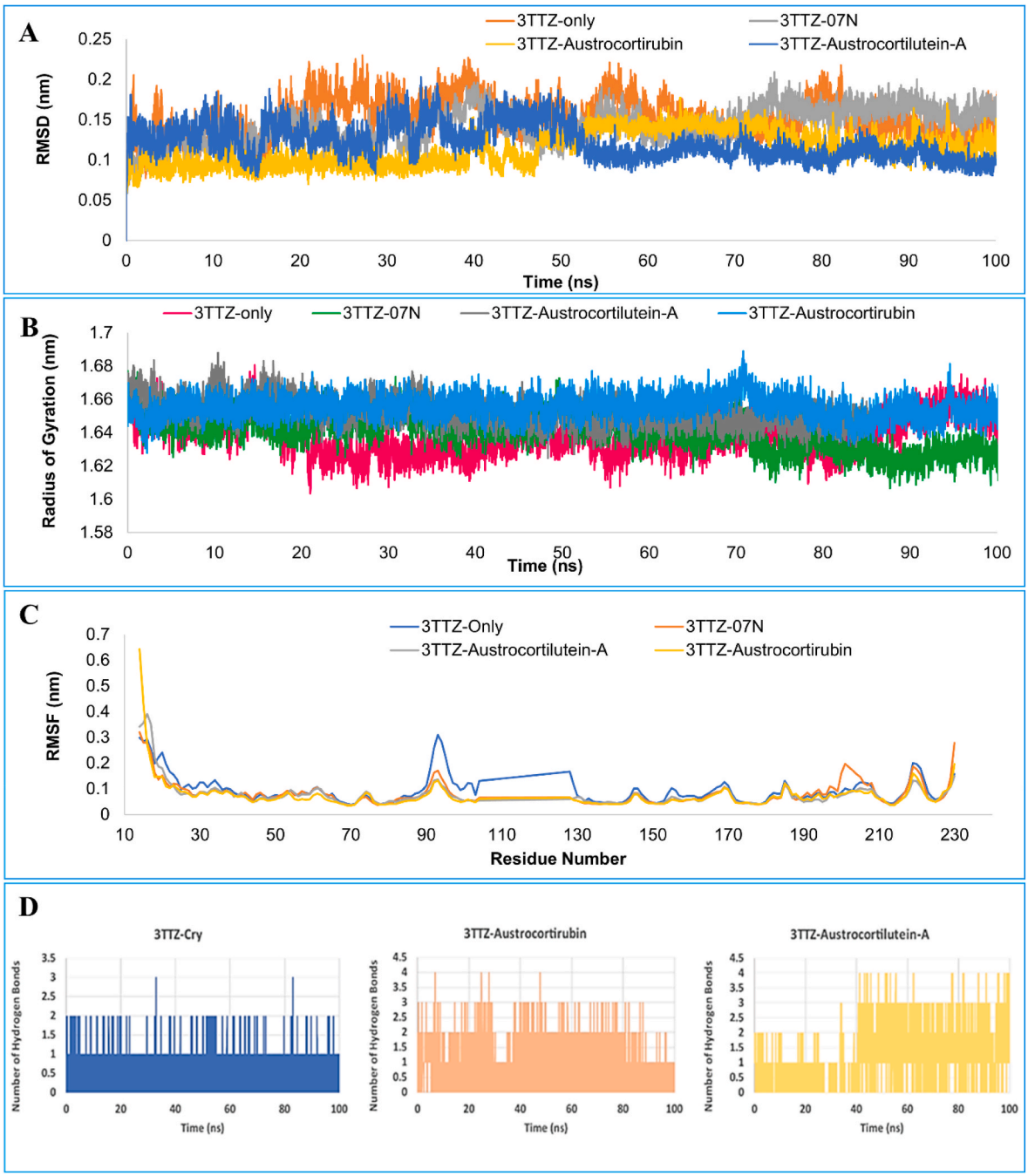

Fig. 6. Molecular dynamics (MD) simulation trajectory analysis of 3TTZ-ligand complexes, (A) RMSD, (B) Radius of Gyration, and (C) RMSF and (D) Hydrogen Bonds. (Note: 07 N refers to the co-crystal ligand of 3TTZ).

4.3. Molecular dynamics simulation

The molecular dynamics simulations for Austrocortilutein A, Austrocortirubin, and Confluentin in complex with their respective target proteins were carried out. The systems were well equilibrated and simulated for 100 ns each, during which they showed the converged metastable states. The results are shown in Table 9. The RMSD of all the 3UDX-ligand systems gradually reached equilibrium within 5 ns and remained stable after that (Fig. 5A). The 3UDX-IM2 complex, which showed the movement of the TG domain towards the TP domain of 3UDX, led to structure compaction, as evidenced by the radius of gyration (Fig. 5B). The RMSF of critical residues were significantly higher in the 3UDX-IM2 complex as compared to 3UDX alone and when in complex with Austrocortilutein A. IM2 formed 3–9 hydrogen bonds with 3UDX while Austrocortilutein A formed 1–3 hydrogen bonds with 3UDX throughout the trajectory. The dominant interactions of IM2 with 3UDX were electrostatic interactions, while in the case of Austrocortilutein A, hydrophobic interactions with 3UDX were dominant. IM2 showed better binding energy (−51.886 kcal/mol) than Austrocortilutein A (−18.8146 kcal/mol), with 3UDX. Confluentin remained bound within the docked cavity until 30 ns, after which it became unstable and exited the pocket due to reduced affinity with the binding site residues of 3UDX. Therefore, further analysis was not carried out.

RMSD of all the 3TTZ-ligand systems gradually increased from 0 to 1 ns and remained stable throughout the trajectory. No significant change was seen in the RMSF of critical residues compared between free and ligand complexed 3TTZ. Reference ligand 07 N formed 1–2 hydrogen bonds, while Austrocortilutein A and Austrocortirubin formed 3–4

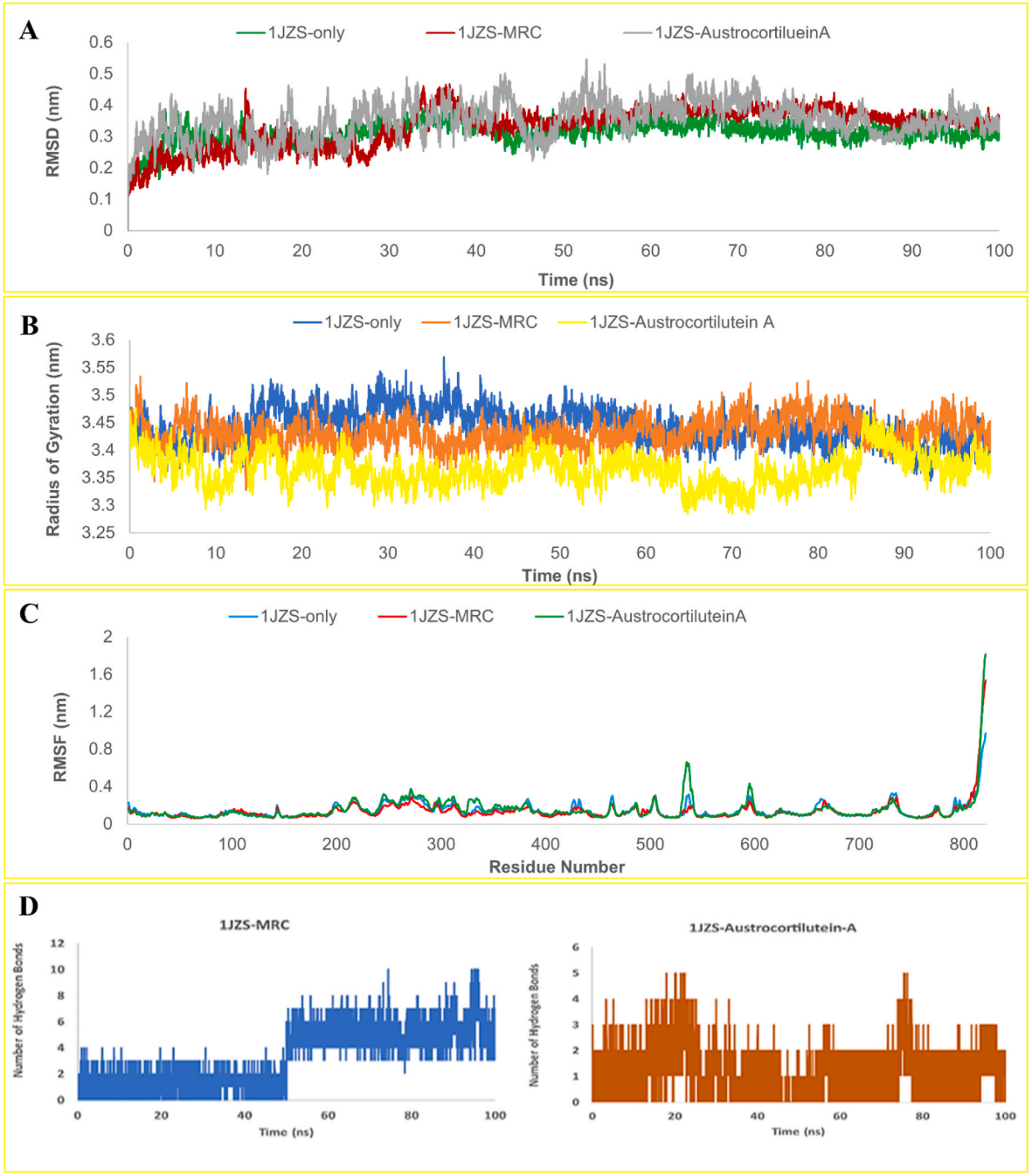

Fig. 7. Molecular dynamics (MD) simulation trajectory analysis of 1JZS-ligand complexes, (A) RMSD, (B) Radius of Gyration, and (C) RMSF and (D) Hydrogen Bonds. (Note: MRC refers to the co-crystal ligand of 1JZS).

hydrogen bonds with 3TTZ throughout the trajectory. Austrocortilutein A (−25.5706 kcal/mol) showed a better binding affinity with 3TTZ, followed by Austrocortirubin (−17.2364 kcal/mol) and 07 N (−8.4081 kcal/mol) (Fig. 6).

RMSD of all the free and ligand complexed 1JZS increased gradually from 0 to 2 ns and then remained stable throughout the trajectory with slight fluctuations. The RMSF of C-terminal loop residues in free and ligand complexed 1JZS was significantly higher than the N-terminal loop residues. The complex of Austrocortilutein A with 1JZS showed slightly higher RMSF in some domains of 1JZS compared to the free 1JZS protein. The reference ligand MRC formed up to 10 hydrogen bonds with 1JZS, while Austrocortilutein A formed up to 5 hydrogen bonds with 1JZS throughout the trajectory. MRC showed better binding affinity (−71.1259 kcal/mol) with 1JZS than Austrocortilutein A (−16.6642 kcal/mol) (Fig. 7).

5. Discussion

Docking scores of the native ligands and the anti-microbial agents are given in Tables 2 and 3, respectively. In the case of 3UDX, the standard ligand was IM2, with an affinity of −6.2 kcal/mol. Based on this score, 2-Aminoquinoline, Austrocortilutein A, Austrocortirubin, Chlorogenic acid, Cinammic, Coloratin A, Confluentin, Ellagic acid, Emodin, Erythroglaucin, Grifolin, Physcion, Quercetin, and Torosachrysone were selected as they had a higher binding affinity. The rest of the compounds were withdrawn due to their similar or lower binding

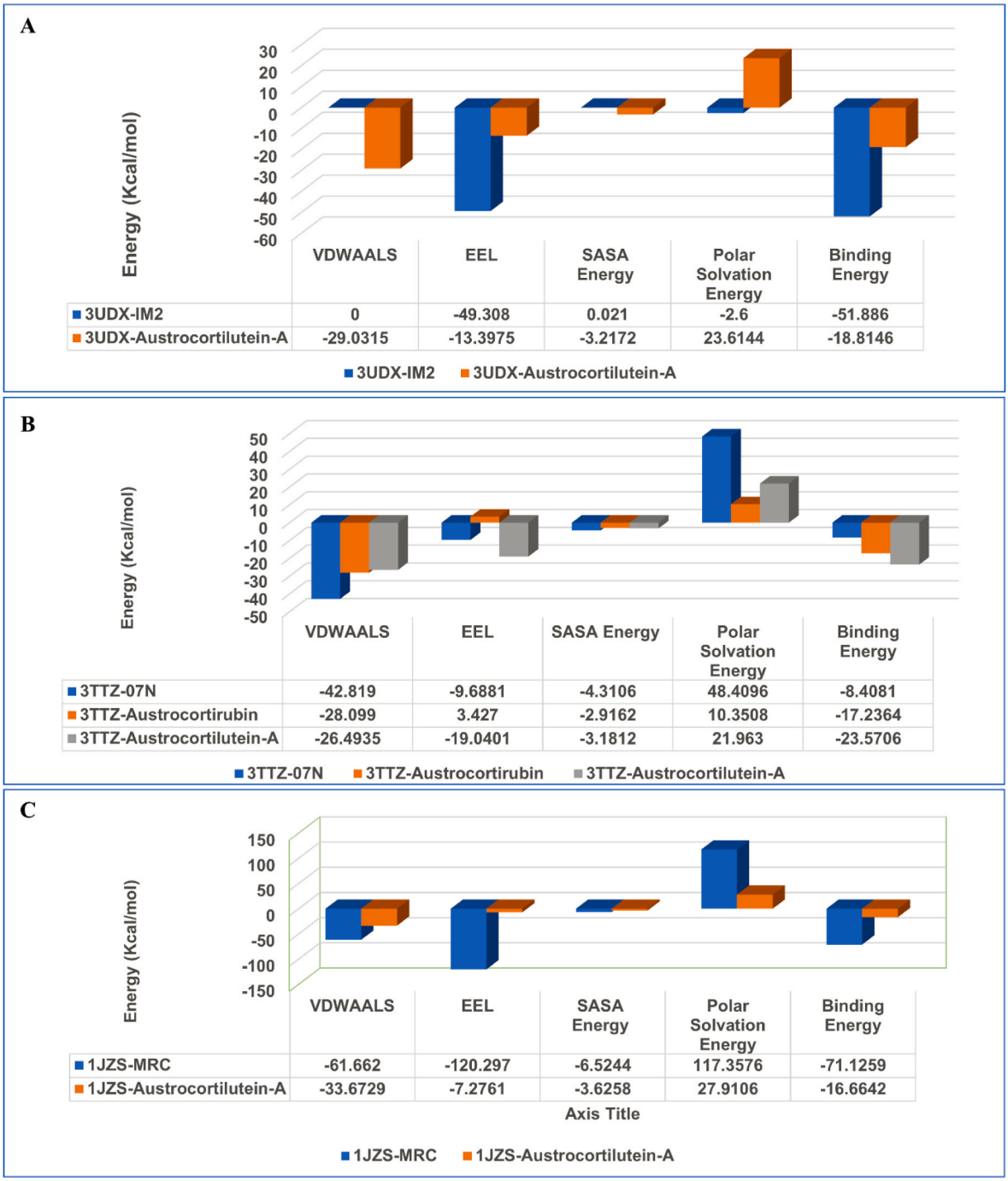

Fig. 8. The end-state binding free-energy calculations of the screened and co-crystal ligands with the target proteins (a) 3UDX, (B) 3TTZ and (C) 1JZS.

affinity compared to the co-crystallized ligand. For native ligand 07 N in 3TTZ, the docking score was −6.8 kcal/mol, and Austrocortilutein A, Austrocortirubin, Chlorogenic acid, Coloratin A, Confluentin, Ellagic acid, Emodin, Erythroglaucin, Grifolin, Ganomycin B, Physcion, Quercetin, and Torosachrysone were selected. Finally, −6.7 kcal/mol was set as the cut-off score for 1JZS, and Austrocortilutein A, Austrocortirubin, Chlorogenic acid, Coloratin A, Confluentin, Cinammic, Ellagic acid, Emodin, Erythroglaucin, Grifolin, Physcion, Quercetin, and Torosachrysone were selected. All these molecules were then subjected to further screening.

MRC-based docking procedure helps to understand receptor flexibility. According to this method, receptor flexibility can generate differences in binding affinity and binding interaction. It also helps us know about the residues that interact most with the ligand and are crucial for forming the drug-receptor complex [53]. Since the crystal structures represent the snapshots of the protein conformation captured at the time of X-ray diffraction, multiple crystal structures of the same protein were used in MRC-based docking to ensure that different conformations of the target proteins are taken into account.

Drug-likeness parameters play an essential role in drug discovery and development. Molecular weight (MW) and topological polar surface area (TPSA) affect the drug permeability across the cell membrane. The lipophilicity of drugs is represented by LogP, which affects the absorption of drugs. A higher value of LogP indicates minimal absorption of the drug. LogS expresses the solubility of the drug, the range being as follows; insoluble < -10; poorly soluble < -6; moderately soluble < -4;

soluble < -2; very soluble <0; highly soluble. Hydrogen bond acceptor (HBA) and hydrogen bond donor (HBD) are supposed to take part in moving the drug substance across the cell membrane. The number of rotatable bonds (RB) is associated with oral bioavailability, and molecules with less than ten rotatable bonds are preferred [54–56]. None of the selected compounds inhibited enzymes of the Cyt P450 family. The inhibition of any of these enzymes indicates a higher chance of drug-drug interaction as it causes problems in the biodegradation and excretion of the drug [57,58].

Pgp in the membrane is associated with the movement of the drug inside the cell, and inhibition of it may hinder the movement [59]. AMES test concerns cancer, and a positive AMES test is associated with mutations indicating that the molecule can act as a carcinogen [60]. Acute oral toxicity indicates adverse effects of a drug that might be induced after taking single or multiple doses of the drug orally within 24h. According to this toxicity index, toxic levels I & II may be fatal, level III may be toxic, and levels IV & V may be harmful if a drug is taken orally (CDER 1996). After considering these factors, Emodin, Erythroglaucin, Physcion, and Quercetin were withdrawn from the list as all these four molecules showed positive AMES toxicity, implying a mutagenic potential. There is high but not complete correspondence between the mutagenicity in the AMES test and the carcinogenicity of compounds in animals. Not all mutations lead to cancer, as the site of the mutation is crucial, and the effect of mutations in the non-coding regions of the genome is most often non-detrimental.

Moreover, Erythroglaucin, Physcion, and Quercetin also showed acute oral toxicity level II, which means they may be harmful if taken orally. Finally, Austrocortilutein A, Austrocortirubin, and Confluentin were shortlisted as their ADMET properties were satisfactory. Although these three molecules are inhibitors of CYP450 1A2 and Austrocortilutein A and Confluentin are inhibitors of CYP450 2C19, there is a possibility of inducing drug-drug interaction if taken with another drug. The inhibition of CYP450 enzymes significantly impacts the development of drugs by altering drug metabolism, pharmacokinetics, and therapeutic efficacy [61]. Inhibition may elevate plasma drug concentrations, thereby increasing toxicity risk and modifying therapeutic benefits, especially for medications with narrow therapeutic indices. Finding possible CYP450 interactions early in the drug development process leads to better screening and dosage adjustments [62]. For drug approval, regulatory bodies require a full assessment of these interactions. The suppression of CYP450 may lead to significant adverse drug responses, particularly in individuals receiving multiple medicines [63].

Various multi-drug-resistant strains of *A. baumannii* have been reported to be resistant even to newer classes of antibiotics, such as imipenem, which create a need to find more potent analogs of currently used antibiotics or novel scaffolds to overcome their anti-microbial resistance. Mahmoud et al. [64] have designed various potent analogs of imipenem against the PBP1a protein of *A. baumannii*. In our study, we tried to target the PBPs group of proteins (PDB: 3UDX), and observed that Austrocortilutein A binds to the *trans*-glycosylase (TG) domain of PBP1a which catalyzes the first step of peptidoglycan synthesis, i.e., polymerization of glycan chains [51]. PBP1a consists of three domains: N terminus glycosyl transfer domain linked to a central transpeptidase (TP) domain through an interdomain linker region and a small C-terminal domain. The TG domains of PBPs play an essential role in resistance against cell-wall targeting antibiotics, and Austrocortilutein A may act as an inhibitor of the TG activity of PBP1a. Austrocortilutein A binds with the TG domain through hydrogen bonding, van der Waals, and hydrophobic interactions with multiple residues, making it a potential anti-PBP1a lead [51,65].

The critical active site residues for the ATP binding domain of DNA Gyrase B include Asp81, Arg84, Gly85, Arg144, and Thr173 [52]. In our study, Austrocortilutein A and Austrocortirubin interacted with the crucial active site residues suggesting the potential applicability of both these molecules as DNA gyrase B inhibitors, and a similar recent study also revealed that multiple analogs of ciprofloxacin bind effectively at the active site of DNA gyrase of *S. aureus* [53]. As per the MDS data, all the 3UDX-ligand systems gradually reached equilibrium within 5 ns and remained stable thereafter. In the case of Austrocortilutein A, 1–3 hydrogen bonds were formed throughout the trajectory while hydrophobic interactions with 3UDX were dominant. The reference ligand IM2 showed better binding energy and stability than Austrocortilutein A with 3UDX; (Fig. 8A). Confluentin remained bound in the docking cavity only for 30 ns and then came out of the pocket and was therefore rejected. These results further support the notion that judging the stability of protein-ligand complex based on only the docking scores might be inaccurate and validation by molecular dynamics simulation is essential.

The MDS results from 3TTZ-ligand systems are encouraging. The reference ligand 07 N formed 1–2 hydrogen bonds, while Austrocortilutein A and Austrocortirubin formed 3–4 hydrogen bonds with 3TTZ throughout the trajectory. Also, Austrocortilutein A and Austrocortirubin exhibited significantly lower binding energies than 07 N (Fig. 8B). The reference ligand MRC formed up to 10 hydrogen bonds and exhibited better binding affinity with 1JZS, while Austrocortilutein A formed up to 5 hydrogen bonds throughout the trajectory, with binding affinity significantly lower than MRC (Fig. 8C). The results of the present work show that in case of the PBP1a and isoleucyl-tRNA synthetase, the lead compound Austrocortilutein A exhibited lower binding affinity than their respective reference ligands IM2 and MRC, but the interaction is stable with multiple hydrogen bonds and hydrophobic interactions. Austrocortilutein A and Austrocortirubin demonstrated better interaction dynamics with DNA gyrase B than the reference ligand. Our results suggest that both lead molecules are worth exploring further in *in vitro* validations.

In the field of drug discovery, the role of medicinal plants and other natural compounds is undeniable. Mushrooms with medicinal properties have been demonstrated to have various pharmacological activities, such as antiallergic, anti-inflammatory, anti-microbial, antioxidative, anti-depressive, GI restoring, antidiabetic, properties as well as being protective for the liver, nervous system, kidneys, bones, etc. Mycotherapy is seen as an expanding field as there are a growing number of studies on the pharmacological potential of the bioactive compounds derived from mushrooms [66,67]. In this research, anti-microbial compounds from mushrooms were computationally evaluated for their binding against the target proteins associated with anti-microbial resistance. After molecular docking and multiple receptor-based dockings, Austrocortilutein A, Austrocortirubin, Confluentin, Ellagic acid, Emodin, Erythroglaucin, Physcion, and Quercetin molecules were shortlisted. Considering the safety factors, the remaining molecules were filtered according to Lipinski's rule of five, and AMDET properties, after which Austrocortilutein A, Austrocortirubin, and Confluentin were selected. The metastability of Austrocortilutein A and Austrocortirubin on the target proteins as evaluated by the molecular dynamics simulations and MMGBSA calculations suggest that these molecules are promising leads and may be further validated.

6. Conclusions

In this study, Austrocortilutein A exhibited good binding affinity in both molecular docking and MRC-based docking to all the groups of target proteins, viz., PBPs, DNA gyrase, and ILERS. At the same time, Austrocortirubin showed a good binding affinity with the DNA gyrase group. Since resistance to natural compounds generally develops slowly, and as shown in MD simulation studies, their stable binding within the binding pockets makes them promising candidates. Both Austrocortilutein A and Austrocortirubin performed better than the positive control against DNA Gyrase B. However, for PBP1a and Isoleucyl-tRNA synthetase, the positive control ligands exhibited better binding affinity, leaving room for further modifications to enhance the potency and selectivity of these mushroom-derived lead compounds. However,

translating computational findings into real-world applications comes with several challenges. Computational models, while useful, may not fully account for the complexity of biological systems, such as protein flexibility, solvent interactions, and post-translational modifications, which can lead to discrepancies between in-silico predictions and actual *in vivo* behavior. Additionally, important factors like bioavailability, toxicity, and pharmacokinetics often require experimental validation, as they are difficult to predict accurately through computational methods alone. Therefore, both *in vitro* and *in vivo* experiments are required to validate the predictions made through this study.

CRediT authorship contribution statement

Gagandeep Singh: Writing – original draft, Visualization, Validation, Software, Methodology, Investigation, Data curation, Conceptualization. **Md Alamgir Hossain:** Writing – original draft, Software, Methodology, Investigation, Data curation, Conceptualization. **Dhurgham Al-Fahad:** Software, Investigation, Data curation. **Vandana Gupta:** Writing – review & editing, Validation, Supervision, Data curation. **Smriti Tandon:** Investigation. **Hemant Soni:** Methodology. **Cheemalapati Venkata Narasimhaji:** Writing – review & editing. **Mariusz Jaremko:** Writing – review & editing, Resources. **Abdul-Hamid Emwas:** Writing – review & editing, Resources. **Md Jamir Anwar:** Writing – review & editing. **Faizul Azam:** Data curation, Validation, Visualization, Writing – review & editing.

Availability of data and materials

The data used is incorporated in the manuscript.

Funding

This research did not receive any specific grant from funding agencies in the public, commercial, or non-profit sectors.

Declaration of competing interest

The authors declare that they have no known competing financial interests or personal relationships that could have appeared to influence the work reported in this paper.

Acknowledgments

The authors acknowledge the High-Performance Computing (HPC) facility at the Indian Institute of Technology Delhi (IIT Delhi), New Delhi, to provide computational resources for conducting the research.

References

[1] F.C. Tenover, Mechanisms of antimicrobial resistance in bacteria, Am. J. Med. 119 (2006) S3–S10.
[2] G. Kapoor, S. Saigal, A. Elongavan, Action and resistance mechanisms of antibiotics: a guide for clinicians, J. Anaesthesiol. Clin. Pharmacol. 33 (2017) 300–305, https://doi.org/10.4103/joacp.JOACP_349_15.
[3] P. Sarkar, V. Yarlagadda, C. Ghosh, J. Haldar, A review on cell wall synthesis inhibitors with an emphasis on glycopeptide antibiotics, Medchemcomm 8 (2017) 516–533, https://doi.org/10.1039/c6md00585c.
[4] J. Calvo, L. Martínez-Martínez, Mecanismos de acción de los antimicrobianos, Enferm. Infecc. Microbiol. Clín. 27 (2009) 44–52, https://doi.org/10.1016/j.eimc.2008.11.001.
[5] D.J. Waxman, J.L. Strominger, PENICILLIN-BINDING proteins and the mechanism of action of beta-lactam antibiotics, Annu. Rev. Biochem. 52 (1983) 825–869, https://doi.org/10.1146/annurev.bi.52.070183.004141.
[6] A.L. Jones, K.M. Knoll, C.E. Rubens, Identification of Streptococcus agalactiae virulence genes in the neonatal rat sepsis model using signature-tagged mutagenesis, Mol. Microbiol. 37 (2000) 1444–1455, https://doi.org/10.1046/j.1365-2958.2000.02099.x.
[7] K.N. Kang, J.M. Boll, PBP1A directly interacts with the divisome complex to promote septal peptidoglycan synthesis in acinetobacter baumannii, J. Bacteriol. 204 (2022) e0023922, https://doi.org/10.1128/jb.00239-22.
[8] A.M. Smith, K.P. Klugman, Alterations in PBP 1A essential-for high-level penicillin resistance in Streptococcus pneumoniae, Antimicrob. Agents Chemother. 42 (1998) 1329–1333, https://doi.org/10.1128/AAC.42.6.1329.
[9] M. Montaner, S. Lopez-Argüello, A. Oliver, B. Moya, PBP target profiling by β-lactam and β-lactamase inhibitors in intact Pseudomonas aeruginosa: effects of the intrinsic and acquired resistance determinants on the periplasmic drug availability, Microbiol. Spectr. 11 (2023) e0303822, https://doi.org/10.1128/spectrum.03038-22.
[10] R. Fontana, G. Cornaglia, M. Ligozzi, A. Mazzariol, The final goal: penicillin-binding proteins and the target of cephalosporins, Clin. Microbiol. Infect. Off. Publ. Eur. Soc. Clin. Microbiol. Infect. Dis. 6 (Suppl 3) (2000) 34–40, https://doi.org/10.1111/j.1469-0691.2000.tb02038.x.
[11] M.A. Kohanski, D.J. Dwyer, J.J. Collins, How antibiotics kill bacteria: from targets to networks, Nat. Rev. Microbiol. 8 (2010) 423–435.
[12] D. Golan, A.H. Tashjian Junior, E.J. Armstrong, A.W. Armstrong, Princípios de farmacologia: a base fisiopatológica da farmacoterapia, in: Princípios de Farmacologia: A Base Fisiopatológica Da Farmacoterapia, 2009, pp. xxiv–952.
[13] O.N. Kostopoulou, T.G. Kourelis, P. Mamos, G.E. Magoulas, D.L. Kalpaxis, Insights into the chloramphenicol inhibition effect on peptidyl transferase activity, using two new analogs of the drug, Open Enzym. Inhib. J. 4 (2011) 1–10.
[14] M. Dadashi, B. Hajikhani, D. Darban-Sarokhalil, A. van Belkum, M. Goudarzi, Mupirocin resistance in Staphylococcus aureus: a systematic review and meta-analysis, J. Glob. Antimicrob. Resist. 20 (2020) 238–247.
[15] X. Yi, J.-L. Liang, P. Wen, P. Jia, S. Feng, S. Liu, Y. Zhuang, Y. Guo, J. Lu, S. Zhong, Giant viruses as reservoirs of antibiotic resistance genes, Nat. Commun. 15 (2024) 7536.
[16] A.C. Spencer, S.S. Panda, DNA gyrase as a target for quinolones, Biomedicines 11 (2023), https://doi.org/10.3390/biomedicines11020371.
[17] S. Rezaei, S. Tajbakhsh, B. Naeimi, F. Yousefi, Investigation of gyrA and parC mutations and the prevalence of plasmid-mediated quinolone resistance genes in Klebsiella pneumoniae clinical isolates, BMC Microbiol. 24 (2024) 265, https://doi.org/10.1186/s12866-024-03383-5.
[18] E. Baekkeskov, O. Rubin, L. Munkholm, W. Zaman, Antimicrobial resistance as a global health crisis. https://doi.org/10.1093/acrefore/9780190228637.013.1626, 2020.
[19] T. Hampton, Report reveals scope of US antibiotic resistance threat, JAMA 310 (2013) 1661–1663.
[20] A. Agarwal, V. Gupta, A.N. Yadav, D. Sain, R.K. Rahi, S.P. Bera, D. Neelam, Aspects of mushrooms and their extracts as natural antimicrobial agents: microbiology, J. Microbiol. Biotechnol. Food Sci. 12 (2023) e9191, https://doi.org/10.55251/jmbfs.9191.
[21] M.J. Alves, I.C.F.R. Ferreira, J. Dias, V. Teixeira, A. Martins, M. Pintado, A review on antimicrobial activity of mushroom (Basidiomycetes) extracts and isolated compounds, Planta Med. 78 (2012) 1707–1718, https://doi.org/10.1055/s-0032-1315370.
[22] R. Kamble, S. Venkata, A.M. Gupte, Antimicrobial activity of Ganoderma lucidum mycelia, J. Pure Appl. Microbiol. 5 (2011) 983–986.
[23] A.M. Younis, F.-S. Wu, H.H. El Shikh, Antimicrobial activity of extracts of the oyster culinary medicinal mushroom Pleurotus ostreatus (higher basidiomycetes) and identification of a new antimicrobial compound, Int. J. Med. Mushrooms 17 (2015).
[24] A. Blagodatski, M. Yatsunskaya, V. Mikhailova, V. Tiasto, A. Kagansky, V. L. Katanaev, Medicinal mushrooms as an attractive new source of natural compounds for future cancer therapy, Oncotarget 9 (2018) 29259–29274, https://doi.org/10.18632/oncotarget.25660.
[25] C.L. Brooks III, D.A. Case, S. Plimpton, B. Roux, D. van der Spoel, E. Tajkhorshid, Classical molecular dynamics, J. Chem. Phys. 154 (2021) 100401, https://doi.org/10.1063/5.0045455.
[26] M.A. Alghamdi, F. Azam, P. Alam, Deciphering Campylobacter jejuni DsbA1 protein dynamics in the presence of anti-virulent compounds: a multi-pronged computer-aided approach, J. Biomol. Struct. Dyn. (2024) 1–17, https://doi.org/10.1080/07391102.2024.2302945.
[27] S. Hug, Classical molecular dynamics in a nutshell, Methods Mol. Biol. 924 (2013) 127–152, https://doi.org/10.1007/978-1-62703-017-5_6.
[28] S.I. Allec, Y. Sun, J. Sun, C.A. Chang, B.M. Wong, Heterogeneous CPU+GPU-Enabled simulations for DFTB molecular dynamics of large chemical and biological systems, J. Chem. Theor. Comput. 15 (2019) 2807–2815, https://doi.org/10.1021/acs.jctc.8b01239.
[29] N. Sepay, S. Chakrabarti, M. Afzal, A. Alarifi, D. Mal, Identification of 4-acrylamido-N-(pyridazin-3-yl)benzamide as anti-COVID-19 compound: a DFTB, molecular docking, and molecular dynamics study, RSC Adv. 12 (2022) 24178–24186, https://doi.org/10.1039/D2RA04333E.
[30] D. Al-Fahad, G. Ropón-Palacios, D.A. Omoboyowa, G. Singh, R.B. Patil, Virtual screening and molecular dynamics simulation of natural compounds as potential inhibitors of serine/threonine kinase 16 for anticancer drug discovery, Mol. Divers. (2024), https://doi.org/10.1007/s11030-024-10931-8.
[31] F. Azam, Elucidation of teicoplanin interactions with drug targets related to COVID-19, Antibiotics 10 (2021) 856, https://doi.org/10.3390/antibiotics10070856.
[32] T. Nakama, O. Nureki, S. Yokoyama, Structural basis for the recognition of isoleucyl-adenylate and an antibiotic, mupirocin, by isoleucyl-tRNA synthetase, J. Biol. Chem. 276 (2001) 47387–47393, https://doi.org/10.1074/jbc.M109089200.
[33] H.M. Berman, J. Westbrook, Z. Feng, G. Gilliland, T.N. Bhat, H. Weissig, I. N. Shindyalov, P.E. Bourne, The protein data bank, Nucleic Acids Res. 28 (2000) 235–242, https://doi.org/10.1093/nar/28.1.235.

[34] W.L. DeLano, Pymol: an open-source molecular graphics tool. CCP4 Newsl, Protein Crystallogr 40 (2002) 82–92.
[35] R. Huey, G.M. Morris, Using AutoDock 4 with AutoDocktools: a tutorial, Scripps Res. Institute. 54 (2008) 56.
[36] S. Kim, P.A. Thiessen, E.E. Bolton, J. Chen, G. Fu, A. Gindulyte, L. Han, J. He, S. He, B.A. Shoemaker, PubChem substance and compound databases, Nucleic Acids Res. 44 (2016) D1202–D1213.
[37] R. Huey, G.M. Morris, S. Forli, Using AutoDock 4 and AutoDock vina with AutoDockTools: a tutorial, Scripps Res. Inst. Mol. Graph. Lab. 10550 (2012) 1000.
[38] O. Trott, A.J. Olson, AutoDock Vina: improving the speed and accuracy of docking with a new scoring function, efficient optimization, and multithreading, J. Comput. Chem. 31 (2010) 455–461.
[39] G. Bottegoni, W. Rocchia, M. Rueda, R. Abagyan, A. Cavalli, Systematic exploitation of multiple receptor conformations for virtual ligand screening, PLoS One 6 (2011) e18845.
[40] J. Hodgson, ADMET—turning chemicals into drugs, Nat. Biotechnol. 19 (2001) 722–726.
[41] F. Cheng, W. Li, Y. Zhou, J. Shen, Z. Wu, G. Liu, P.W. Lee, Y. Tang, admetSAR: a comprehensive source and free tool for assessment of chemical ADMET properties, J. Chem. Inf. Model. 52 (2012) 3099–3105, https://doi.org/10.1021/ci300367a.
[42] BIOVIA, Dassault Systèmes, Discovery Studio Visualizer, Dassault Systèmes, San Diego, 2020, p. n.d.. No Title, version 20.1.0.19295.
[43] L.P. Kagami, G.M. das Neves, A.W.S. da Silva, R.A. Caceres, D.F. Kawano, V. L. Eifler-Lima, LiGRO: a graphical user interface for protein-ligand molecular dynamics, J. Mol. Model. 23 (2017) 304, https://doi.org/10.1007/s00894-017-3475-9.
[44] M.J. Abraham, T. Murtola, R. Schulz, S. Páll, J.C. Smith, B. Hess, E. Lindahl, GROMACS: high performance molecular simulations through multi-level parallelism from laptops to supercomputers, SoftwareX 1–2 (2015) 19–25, https://doi.org/10.1016/j.softx.2015.06.001.
[45] K. Lindorff-Larsen, S. Piana, K. Palmo, P. Maragakis, J.L. Klepeis, R.O. Dror, D. E. Shaw, Improved side-chain torsion potentials for the Amber ff99SB protein force field, Proteins 78 (2010) 1950–1958, https://doi.org/10.1002/prot.22711.
[46] V.H. Man, X. He, P. Derreumaux, B. Ji, X.-Q. Xie, P.H. Nguyen, J. Wang, Effects of all-atom molecular mechanics force fields on amyloid peptide assembly: the case of aβ(16-22) dimer, J. Chem. Theor. Comput. 15 (2019) 1440–1452, https://doi.org/10.1021/acs.jctc.8b01107.
[47] S.A. Showalter, R. Brüschweiler, Validation of molecular dynamics simulations of biomolecules using NMR spin relaxation as benchmarks: application to the AMBER99SB force field, J. Chem. Theor. Comput. 3 (2007) 961–975, https://doi.org/10.1021/ct7000045.
[48] A.W. Sousa da Silva, W.F. Vranken, Acpype - AnteChamber PYthon parser interfacE, BMC Res. Notes 5 (2012) 367, https://doi.org/10.1186/1756-0500-5-367.
[49] M.S. Valdés-Tresanco, M.E. Valdés-Tresanco, P.A. Valiente, E. Moreno, gmx_MMPBSA: a new tool to perform end-state free energy calculations with GROMACS, J. Chem. Theor. Comput. 17 (2021) 6281–6291, https://doi.org/10.1021/acs.jctc.1c00645.
[50] H.K. Permatasari, F. Nurkolis, H. Hardinsyah, N.A. Taslim, N. Sabrina, F. M. Ibrahim, J. Visnu, D.A. Kumalawati, S.A. Febriana, T. Sudargo, Metabolomic assay, computational screening, and pharmacological evaluation of Caulerpa racemosa as an anti-obesity with anti-aging by altering lipid profile and peroxisome proliferator-activated receptor-γ coactivator 1-α levels, Front. Nutr. 9 (2022) 939073.
[51] S. Han, N. Caspers, R.P. Zaniewski, B.M. Lacey, A.P. Tomaras, X. Feng, K. F. Geoghegan, V. Shanmugasundaram, Distinctive attributes of β-lactam target proteins in acinetobacter baumannii relevant to development of new antibiotics, J. Am. Chem. Soc. 133 (2011) 20536–20545, https://doi.org/10.1021/ja208835z.
[52] M.F. Mesleh, J.B. Cross, J. Zhang, J. Kahmann, O.A. Andersen, J. Barker, R. K. Cheng, B. Felicetti, M. Wood, A.T. Hadfield, Fragment-based discovery of DNA gyrase inhibitors targeting the ATPase subunit of GyrB, Bioorg. Med. Chem. Lett. 26 (2016) 1314–1318.
[53] M.R. Hasan, S.M. Chowdhury, M.A. Aziz, A. Shahriar, H. Ahmed, M.A. Khan, S. Mahmud, T. Bin Emran, In silico analysis of ciprofloxacin analogs as inhibitors of DNA gyrase of Staphylococcus aureus, Inform. Med. Unlocked 26 (2021) 100748.
[54] C.A. Lipinski, Lead-and drug-like compounds: the rule-of-five revolution, Drug Discov. Today Technol. 1 (2004) 337–341.
[55] M.P. Pollastri, Overview on the rule of five, Curr. Protoc. Pharmacol. 49 (2010) 9–12.
[56] T. Sander, OSIRIS property explorer, Org. Chem. Portal (2001). https://www.organic-chemistry.org/prog/peo/. (Accessed 12 September 2023).
[57] F.P. Guengerich, Cytochrome P-450 3A4: regulation and role in drug metabolism, Annu. Rev. Pharmacol. Toxicol. 39 (1999) 1–17.
[58] A.P. Li, Screening for human ADME/Tox drug properties in drug discovery, Drug Discov. Today 6 (2001) 357–366.
[59] K.M.R. Srivalli, P.K. Lakshmi, Overview of P-glycoprotein inhibitors: a rational outlook, Brazilian J. Pharm. Sci. 48 (2012) 353–367.
[60] K. Mortelmans, E. Zeiger, The Ames Salmonella/microsome mutagenicity assay, Mutat. Res. Mol. Mech. Mutagen. 455 (2000) 29–60.
[61] S. Armani, A. Geier, T. Forst, U. Merle, D.H. Alpers, M.W. Lunnon, Effect of changes in metabolic enzymes and transporters on drug metabolism in the context of liver disease: impact on pharmacokinetics and drug–drug interactions, Br. J. Clin. Pharmacol. 90 (2024) 942–958, https://doi.org/10.1111/bcp.15990.
[62] L. Xu, B. Das, C. Prakash, CYP450 enzymes in drug discovery and development: an overview, in: Encyclopedia of Drug Metabolism and Interactions, 2012, pp. 1–35, https://doi.org/10.1002/9780470921920.edm117.
[63] J. Hakkola, J. Hukkanen, M. Turpeinen, O. Pelkonen, Inhibition and induction of CYP enzymes in humans: an update, Arch. Toxicol. 94 (2020) 3671–3722, https://doi.org/10.1007/s00204-020-02936-7.
[64] A. Mahmoud, M.M. Afifi, F. El Shenawy, W. Salem, B.H. Elesawy, Syzygium aromaticum extracts as a potential antibacterial inhibitors against clinical isolates of acinetobacter baumannii: an in-silico-supported in-vitro study, Antibiotics 10 (2021) 1062.
[65] C. Contreras-Martel, V. Job, A.M. Di Guilmi, T. Vernet, O. Dideberg, A. Dessen, Crystal structure of penicillin-binding protein 1a (PBP1a) reveals a mutational hotspot implicated in beta-lactam resistance in Streptococcus pneumoniae, J. Mol. Biol. 355 (2006) 684–696, https://doi.org/10.1016/j.jmb.2005.10.030.
[66] Lallawmsanga, A.K. Passari, V.K. Mishra, V.V. Leo, B.P. Singh, G. Valliammai Meyyappan, V.K. Gupta, S. Uthandi, R.C. Upadhyay, Antimicrobial potential, identification and phylogenetic affiliation of wild mushrooms from two sub-tropical semi-evergreen Indian forest ecosystems, PLoS One 11 (2016) e0166368.
[67] G. Venturella, V. Ferraro, F. Cirlincione, M.L. Gargano, Medicinal mushrooms: bioactive compounds, use, and clinical trials, Int. J. Mol. Sci. 22 (2021) 634.